Study of the Effect of Local Forcing on the Fractal Behavior of Shallow Groundwater Levels in a Riparian Aquifer

Abrar Habib[1], Athanasios Paschalis[2], Christian Onof[2], John P. Bloomfield[3], James P. R. Sorensen[3], Adrian P. Butler[2]

[1] Civil Engineering Department, University of Bahrain, Kingdom of Bahrain

[2] Department of Civil and Environmental Engineering, Imperial College London, London, SW7 2AZ, UK

[3] British Geological Survey, Maclean Building, Crowmarsh Gifford, Wallingford, Oxon, OX10

Corresponding Author: Abrar Habib (abr.habib@gmail.com / amhabib@uob.edu.bh)

Abstract

With the help of a physically based recharge-groundwater flow model and robust detrended fluctuation analysis (r-DFAn), the effect of local (catchment-scale) forcing on groundwater levels' scaling behavior in a riparian aquifer in Wallingford, UK, is investigated. The local forcings investigated in this study include the rainfall's temporal scaling behavior (which is simulated by changing rainfall's intermittency parameter in a β -lognormal multiplicative random cascade model), the aquifer's physical parameters (saturated hydraulic conductivity, specific yield, the empirical coefficients of the water retention curve, and the river stage's scaling behavior).

Groundwater level's scaling behavior was found to be most sensitive to rainfall's fractal behavior. Additionally, there is preliminary evidence suggesting that changes to the rainfall's local scaling behavior (i.e., change to the series' scaling that induces crossovers) affects the groundwater's and the recharge's local scaling behavior.

Keywords: Groundwater levels' fractal behavior, multiplicative random cascade model, drainage fractal behavior

1. INTRODUCTION

The property of self-affinity or fractal behavior is a peculiar property that makes smaller parts of an object identical to the whole (Mandelbrot, 1982). This occurs in many objects in nature, like trees, leaves, mountains, clouds, etc. Variables in the field of water resources are also fractal in nature; but this property is observed in time, as opposed to space, and the assessment of similarity is with statistical relationships of the time series rather than geometric similarity. Since the fractal behavior of a time series indicates how the time series' statistics depend on scale, it has various implications in water resources management. A major one is the level of persistence of a series, i.e., its likelihood to remain at its current value (Williams & Pelletier, 2015). Depending on the time series, the implications of this may vary. In water resources management, the likelihood of a variable remaining at a high or a low value is important when studying flood risks or planning for potential dry periods or droughts (Habib, A., 2020).

In the field of hydrology, the fractal behavior of hydrological time series has long been acknowledged (Kantelhardt et al., 2001; Li & Zhang, 2007; Little & Bloomfield, 2010; Matsoukas, Islam & Rodriguez-Iturbe, 2000). It is a 'fundamental hidden order' (National Research Council, 1991), i.e. a property that is inherent in hydrological time series that can be quantified but not necessarily visually noticed. Simulating this 'fundamental hidden order' and studying the factors that affect it provides insights into the processes and variables being simulated. For this reason, among others, researchers have gained interest in modelling and studying fractal behavior. Various researchers have modelled the fractal behavior of hydrological and other variables by converting simple and known models from the time-space domains to the spectral domain (refer to the supplementary material), and others, more recently, used physically-based models in the time domain to simulate hydrological (or related) variables while incorporating fractal behavior of the system being modelled by analysing the outputs and/or inputs using various known techniques (with power spectral analysis being the most commonly used). This helped them gain insights into the variables/processes being modelled (refer to the supplementary material).

A non-exhaustive list is presented in chronological order in the supplementary material to present a general picture of previous efforts for using models to incorporate or simulate fractal behavior. Spectral analysis is the preferred method of most researchers, whether for representing the entire hydrological process in the frequency domain (Gelhar, 1974), or simply analyzing the input and/or output time series using Fourier transform.

In this work a physically based model is used to study the fractal behavior of groundwater levels. However, the novelty of this work lies, firstly, in the use of robust detrended fluctuation analysis, r-DFAn (Habib, A. et al., 2017), to objectively study the fractal behavior of groundwater levels and the fractal behavior of the input forcing. This enables reliable comparison between various series, and it enables the systematic study of changes to the scaling regime (which will be referred to as ‘local scaling behavior’). Secondly, rainfall series of varying fractal properties are simulated and used to drive the physically based model and the benefits of this are addressed in the relevant section below.

2. METHODOLOGY

2.1 Study Site

The study site is located in Wallingford, United Kingdom (Figure 1), and it comprises a shallow riparian aquifer, about 5m depth, with groundwater levels that fluctuate over a wide variety of time scales. The monitored data include high resolution 1-minute groundwater levels and river stage, 15-minute rainfall, among other meteorological variables, all of which are summarized in Table 1, and the gauge locations are indicated in Figure 1. The available data cover 4 years between January 2012 and January 2016.

[insert figure 1]

[insert table 1]

2.2 Fractal Behavior Quantification

The data have been analyzed for fractal behavior using robust detrended fluctuation analysis (r-DFAn) (Habib, A. et al., 2017). r-DFAn is a recently developed procedure that utilizes the well-known detrended fluctuation analysis (Peng et al., 1994) and a number of statistical models to estimate reliable scaling behavior. The statistical models used were robust regression, to estimate a global scaling exponent as explained in Figure 2, piecewise linear regression to estimate optimum crossover locations, analysis of covariance (ANCOVA) to determine whether the local scaling exponents (explained in Figure 2) were statistically different or not, and multiple comparison procedure to enable comparing three or more groups of data, which is the case when having three or more local scaling exponents. A detailed explanation of r-DFAn can be found in (Habib, A. et al., 2017).

[Insert fig 2]

2.3 Groundwater Levels Simulation

Groundwater levels at the study-site are simulated using a recharge-groundwater flow model (Habib, Abrar et al., 2022). The model comprises of a Soil Moisture Accounting Procedure (SMAP) to simulate recharge (Mathias et al., 2015), and a 1D non-linear partial differential equation (the Boussinesq Equation) to simulate groundwater levels with a no-flow boundary at one end and a time-varying specified head boundary at the River Thames. The model is written in MATLAB with explicit discretization for the SMAP, which is derived from a simple water balance integrated over the depth of a soil column (Mathias et al., 2015), and implicit discretization of the Boussinesq Equation (Habib, Abrar et al., 2022). Potential evapotranspiration is estimated from the meteorological data monitored in Wallingford using the procedure explained in FAO Irrigation and Drainage Paper 56 (Allen, et al, 1998). A total of 14 parameters are included in the sensitivity analysis. The sensitivity analysis is performed using Latin Hypercube sampling which involved a total of 12,000 model runs. As a result, 6 parameters are identified as sensitive (showed in Figure 3). Multi-objective optimization using a pattern search algorithm (Custódio et al., 2011) is used to determine the non-dominated parameter sets of the sensitive parameters. A total of 21 unique non-dominated parameter sets are identified. A mathematical representation of the model, the sensitivity analysis and optimization are presented in detail in (Habib, Abrar et al., 2022). A summary of the workings of the model along with the input series and sensitive parameters is presented in Figure 3. The model runs at a spatial resolution of 5m and a temporal resolution of 15 minutes.

[insert fig 3]

The non-dominated (i.e. optimum) groundwater level simulations are presented in Figure 4, however, for the purpose of this research, one of these time series will be selected based on its performance in the fractal domain (i.e. its r-DFAn results). The selected GWL simulation is shown in Figure 4 and its fractal behavior is presented in Figure 5. The selected simulation has a Nash Sutcliff Efficiency of 0.716.

[insert fig 4]

[insert fig 5]

The objective of this work is to investigate which forcing affects the fluctuation structure of groundwater levels in Wallingford. Hence, the recharge-groundwater flow model, with the selected optimum parameter set, is used to simulate groundwater levels while varying the input time series and parameters as explained below. The selected inputs and parameters, which will be varied, are highlighted in Figure 3 in orange and the fractal behavior of the simulated groundwater levels will be analyzed using r-DFAn.

The procedure adapted for varying the parameters and input series is as follows:

- The selected optimum parameter values will be rescaled within certain limits that are found to produce reasonable groundwater levels in both time and fractal domains,
- A random permutation of river stage will be used as the downstream specified head boundary instead of the observed river stage series to run the recharge-groundwater flow model. This will break the temporal structure of the time series and result in white noise. Two simulated groundwater series will be generated - one with the observed river stage and the other with the random permutation. This will enable testing of the effect of river stage's fractal behavior (i.e., the value of its scaling exponent) on groundwater levels, and
- finally, the recharge-groundwater flow model will be forced by rainfall input series with different fractal properties, which have varying global scaling exponents as explained in section 2.2.

The rainfall model used to generate rainfall realizations with different fractal behavior is explained in the following section.

2.4 Stochastic Rainfall Model

The β-lognormal model used in (Molnar & Burlando, 2008; Over & Gupta, 1994; Paschalis, Molnar & Burlando, 2012), which is a discrete multiplicative random cascade, will be used to downscale different realizations of the observed rainfall series. This is done by aggregating observed series to a daily time scale and then using the cascade generator for downscaling. The cascade generator (w) is described as follows (Over, 1995):

$$w = w_{\beta} w_{log\,n} \tag{1}$$

where w_{β} is the β model's cascade generator and $w_{log\,n}$ is the lognormally distributed cascade generator of the lognormal model and both are computed as follows (Over & Gupta, 1994; Over, 1995):

$$w_{\beta} = \begin{cases} 0\; with\, probability\;\; p = 1 - 2^{-\beta} \\ 2^{\beta}\; with\, probability\;\; 1 - p = 2^{-\beta} \end{cases} \tag{2}$$

$$w_{log\,n} = 2^{\mu + \sigma X} \tag{3}$$

where μ and σ are, respectively, the mean and variance of the lognormal cascade generator ($w_{log\,n}$) and X is a standard Gaussian random variable. To preserve the mean of the generated rainfall series when downscaling, μ and σ are not independent. β and σ are essential for describing the scaling field of the rainfall series, and it is from observed rainfall's scaling field that the parameters are calibrated (Molnar & Burlando, 2008). The β parameter indicates the level of intermittency of the generated rainfall series (Molnar & Burlando, 2008).

In this context, the performance of the rainfall model is assessed based on its ability to preserve observed rainfall's basic statistical properties such as its mean, standard deviation, probability of dry periods and its distribution. The assessment of the model's performance is performed at a number of aggregation scales as shown in Figure 6. The performance of the model was found satisfactory for simulating rainfall at Wallingford. It should be noted that due to the discrete nature of the multiplicative random cascade, there is an overestimation of the probability of no-rainfall at the daily scale. The reason is that there is a non-zero probability that the downscaled rainfall is zero (e.g. if the first 2 multiplicative weights w_{β} are both zero), even if the rainfall depth at the daily scale where the downscaling procedure started, is not.

[insert fig 6]

Following the calibration, the stochastic rainfall model is used to simulate various rainfall series of different fractal behavior, and this is done by changing the values of the calibrated parameters. Results of this exercise, in addition to other results, are presented in the following section.

3. RESULTS

The aim of this study is to explore the impact of altering the time series and parameters that drive the coupled recharge-groundwater flow model on the fractal behavior of the simulated groundwater levels. To achieve this the time series or parameters are modified one-at-a-time, while holding the others constant, to see which local forcing has an effect on the groundwater level's fractal behavior. This sensitivity analysis of the fractal behavior of the simulated groundwater levels is performed in the time domain and using a physically based model which will help relate changes in the fractal behavior to physical phenomena. Table 2 summarizes all the parameters included in the analysis that follows.

The effect of the following on groundwater levels' fractal behavior in the Wallingford study site is studied:

- Rainfall's fractal behavior.
- Aquifer's physical properties. These include the hydraulic conductivity and specific yield of the shallow unconfined aquifer in Wallingford.
- Empirical parameters in the Van-Genuchten-Mualem Model describing the water retention curve.
- River stage's fractal behavior and its distance from the borehole at which GWLs are observed.

[insert table 2]

Based on the results, we have divided the above time series/parameters into two main categories: sensitive ones and non-sensitive ones. Sensitive factors are those that produce statistically different fractal behavior in groundwater levels and vice versa are the non-sensitive factors. Rainfall fractal behavior resulted in statistically significant change in the groundwater levels' global fractal behavior. The remaining factors did not. The results are presented in the following sub-sections and a discussion of the results are presented in Section 4.

3.1 Sensitive Factors - Rainfall

Using the stochastic rainfall model, different values of the intermittency parameter β are used to simulate rainfall series of varying fractal properties. By altering the β parameter we focus on the scaling of the probability of zero rainfall. For every change in the β parameter, 5 realisations are simulated. A total of 40 rainfall realisations are simulated with resulting global scaling behavior ranging from 0.6 to 1.05. Figure 7 presents a number of simulated groundwater level series using simulated rainfall. The range of β parameters is large enough such that intensities at the lowest scale between extreme case simulations differ significantly. Rainfall amounts at the daily scale are, for all simulations, preserved on average.

[insert fig 7]

The 40 rainfall realizations are used to drive the coupled recharge-groundwater flow model to simulate 40 drainage series and 40 groundwater levels. Figure 8 presents a summary of the global scaling exponents of all simulated rainfall realizations and corresponding drainage and groundwater levels.

[insert fig 8]

Looking further into the effect of rainfall's fractal behavior, we find that changes to the rainfall's global scaling exponent strongly affect the fractal behavior of drainage. This is evident from Figure 9 when comparing the slopes which describe the change of global scaling exponent of each variable relative to changes in rainfall's global scaling exponent, where changes in the global scaling exponents of drainage are significantly larger than those of both rainfall and groundwater levels.

[insert fig 9]

On one hand, global fractal behavior is quantified using the global scaling exponent which describes the slope of the change of variance change across all studied scales of a series (on a double logarithmic plot) as explained in section 2.2. On the other hand, there may be instances of local scaling behaviors which refer to changes in the scaling exponents across certain scales. These result in crossovers or breakpoints in the fractal behavior (as illustrated in Figure 2). The *local* fractal behavior of rainfall on both drainage and groundwater levels is investigated. This is done by exploring the degree of correlation between rainfall's local fractal behavior and that of both drainage and groundwater levels.

Local fractal behavior is described in terms of local scaling exponents and crossovers. Relating crossover locations is difficult because the number of crossovers is seldom equal in the series being compared, and hence, crossovers in two series cannot always be associated with each other. Local scaling exponents extend over different ranges of scales, and hence, comparing local scaling exponents is not straightforward either. This is illustrated in the left panel of Figure 10 where neither crossovers nor local scaling exponents in series A can be individually associated to those in series B. Hence, as illustrated in Figure 10, the r-DFA plot is transformed into a different series that contains information about the local scaling exponent and the range of scales over which it extends (hence indirectly reflecting the crossover location). The correlation coefficient of the transformed series is then determined and the results of the 40 rainfall realizations and its corresponding drainage and groundwater levels are presented in Figure 11. The correlations between rainfall and drainage, rainfall and groundwater levels, and drainage and groundwater levels are determined.

[insert fig 10]

60%, 70% and 80% of the correlation coefficients determined between, respectively, rainfall and drainage, rainfall and groundwater levels, and drainage and groundwater levels, are higher than 0.7 (Figure 11). The bottom illustration in Figure 11 summarizes the correlation coefficients determined. They all lie towards the higher end of correlations with the correlations between drainage and groundwater levels significantly different than the other two correlation groups (evident from the non-overlapping confidence intervals).

[insert fig 11]

3.2 Non-Sensitive Factors

3.2.1 Hydraulic Conductivity and Specific Yield

The hydraulic conductivity and specific yield are varied in the range between 50% and 500%. As mentioned before, changes are made to one parameter at a time and the optimized parameter value is used as the starting point. The range of variation depends on typical parameter values known to be acceptable for the study site Figure 12 presents the results. The bottom panels in Figure 12 present the r-DFA1 plots for the various hydraulic conductivity and specific yield values used.

[insert fig 12]

3.2.2 Recharge Parameters

The same methodology is used for the aquifer's physical parameters are applied to the recharge parameters. The recharge parameters are varied between 25% and 175% of the optimized values. This range was found to produce groundwater levels that are acceptable given the aquifer's dimensions and the river levels. The recharge parameters (referred to as m and η) are empirical parameters from the Van Genuchten-Maulem Model used in the SMAP recharge model (Habib, Abrar et al., 2022; Van Genuchten, 1980). Figure 13 presents the results.

[insert fig 13]

3.2.3 River Stage's Fractal Behavior and Distance from Groundwater Level Measurements

The impact of river stage on groundwater levels' fractal behavior is studied in two ways. Firstly, the observed river stage series is randomly shuffled to break its scaling structure while maintaining the original distribution of the series. Groundwater levels are simulated using this series at the river boundary. It is observed that this did not affect groundwater levels that are monitored at a distance of 420m from the river. This indicates that the fractal behavior of river stage does not impact groundwater levels at this distance. Secondly, groundwater levels are simulated at various distances from the river while using the observed river stage at the specified head boundary. The results are presented in Figure 14.

[insert fig 14]

4. DISCUSSION

In this section, we discuss the results, compare the findings with current literature and recommend further investigations that may be a part of future work.

4.1 Sensitive Factors - Rainfall

The results for rainfall are presented in Section 3.1. It is noteworthy that rainfall realizations for different β parameters, shown in Figure 8, have statistically different global scaling exponents and these in turn produce statistically different global scaling exponents for both drainage and groundwater levels. Furthermore, simulations with $\beta \times 1.0$, i.e. with no change to the calibrated values, result in values of global scaling exponents that are similar to the observed values, which validates the simulated rainfall.

We then look at the change of scaling exponents for drainage rates and groundwater levels in comparison with the rate of change of scaling exponents of rainfall (Figure 9). We find that the rate of change of the drainage scaling exponents is higher than those of both rainfall and groundwater levels. This is attributed to the unsaturated zone which magnifies the effect of extended dry periods in the case of an intermittent rainfall signal or wetter circumstances in the case of a less intermittent rainfall signal. In addition, although the absolute global scaling factors for groundwater levels are larger than those for both rainfall and drainage, it is significant that the rate of change in these values is about double that of rainfall and around two-thirds of recharge. This highlights the complexity of the role of the unsaturated zone and how the temporal fractal properties of rainfall are modified as water moves through the unsaturated zone and into the near-surface groundwater system.

A novel finding is the effect of change of global fractal behavior of rainfall series on that of drainage/recharge and groundwater levels. Previous publications have highlighted the increase in memory of a white noise or observed rainfall series as it infiltrates through soil (Gelhar, 1974; Yang, Zhang & Liang, 2017; Zhang & Schilling, 2004), however, comparing the degree of change of global fractal behavior between rainfall, drainage and groundwater levels has, to the best of our knowledge, not been investigated previously.

Figure 11 shows evidence that the local fractal behavior in rainfall may affect local fractal behavior in both drainage and groundwater levels. However, it is interesting to observe that the local scaling behavior correlation between drainage and groundwater is statistically stronger than the other two sets. Our hypothesis is that this is due to the fact that all of the groundwater series and most of the drainage series have global scaling exponents greater than 1.05, which is the critical threshold referred to in (Habib, A., 2020) above which the physical meaning of persistence is pronounced. In other words, the memory of series exhibiting global scaling exponents greater than ~1.05 persists longer on dry or wet periods as opposed to series with global scaling exponents less than ~1.05, such as the rainfall series. Hence local scaling behavior which is affected by drier or wetter days, weeks and months are more correlated between drainage and groundwater series.

4.2 Non-Sensitive Factors

4.2.1 Hydraulic Conductivity, Specific Yield and the Recharge Parameters

Contrary to speculation that the fractal behavior of groundwater depends on the aquifer's physical properties (Li & Zhang, 2007; Yu et al., 2016; Zhang & Schilling, 2004), results from the Wallingford site using a recharge-groundwater flow model shows that varying the physical parameters –namely hydraulic conductivity and specific yield – over a range of 50% to 500% does not produce differences in the global fractal behavior of groundwater levels that is statistically significant (top panels in Figure 12). It is important to note, however, that results may differ for other study sites with different geological and geometric properties.

Although there is no significant change in the global fractal behavior of groundwater levels, for hydraulic conductivity (bottom left panel in Figure 12), there is a slight change at larger timescales, i.e., for periods greater than a few days. In contrast, increases in specific yield, as depicted in Figure 12 bottom right panel, lead to a general reduction in the variance of groundwater levels. This reduction in variance is constant over all scales due to the minor change in the global fractal behavior of groundwater levels. This is not surprising given the additional storage an increase in Sy provides. This additional storage, in turn, damps down groundwater fluctuations and hence leads to a reduction in F(L) values across all timescales.

As for the unsaturated zone parameters, which affect recharge, Figure 13 (top left and right) shows the overlapping confidence intervals of the global scaling exponents of groundwater levels that are simulated using different recharge parameters. The m recharge parameter affects smaller timescales (i.e less than a day) in the groundwater levels scaling behavior (bottom left panel in Figure 13), which is reported in literature (Katul et al., 2007). The effect of the m recharge parameter is contrary to the effect of hydraulic conductivity, which affects the larger scales only, as indicated in Figure 12. Varying the η parameter does not appear to have any effect on groundwater levels local fractal behavior (bottom right panel Figure 13).

4.2.2 River Stage's Fractal Behavior and Distance from Groundwater Level Measurements

As mentioned in section 3.2.3, the effect of the river levels, after breaking its fractal structure by randomly shuffling it, showed no effect at the distance at which groundwater levels are measured (420m from the river).

Next, the effect of river stage on groundwater levels at different distances is studied (Figure 14). Groundwater levels closer to the river, in the vicinity of 100m, showed a small change to global fractal behavior in response to the change in the river stage's fractal behavior (Figure 14 middle panel). Notable, as well, is the reduction in fractal behavior of groundwater levels to values lower than that of the river. This is explained by the fact that the flow of groundwater computed by the combined recharge-groundwater flow model is governed solely by change in head gradient (Darcy's Equation) and the complex dynamics at the river-aquifer interface are not modelled. Hence, at close vicinity to the river, fluctuation of river stage may result in reverse flows (i.e. flow from the river into the aquifer) during some periods as shown in the simulated time series in the top panel of Figure 14, which, may not be the case in reality. It is expected that in reality the global fractal behavior of groundwater levels would not be lower than that of river stage (Little & Bloomfield, 2010). Figure 14 also shows that the groundwater level's local fractal behavior is affected mainly across larger scales, especially for groundwater levels closer to the river and this is similar to previously published results (Liang & Zhang, 2013).

5. SUMMARY, CONCLUSIONS AND RECOMMENDATIONS

A physically-based recharge-groundwater flow model, that was developed, calibrated and assessed in both time and fractal domains for a riparian aquifer in Wallingford, United Kingdom (Habib, Abrar et al., 2022), has been used here to study the sensitivity of groundwater levels' fractal behavior to various forcings and parameters required to run the model. The forcings and parameters considered were rainfall's fractal behavior, the aquifer's physical parameters, the empirical parameters for simulating recharge, the river stage's fractal behavior and its distance from the observation borehole.

It was found that changes to the rainfall's fractal behavior –simulated by changing the rainfall's intermittency in a stochastic rainfall model, – was the only factor that resulted in statistically different global fractal behavior of groundwater levels. This result appears to be due to the marked change in the fractal behavior of groundwater recharge. Such a result provides an important insight into the controls on the fractal behavior of groundwater levels and one which could benefit from further investigation.

Using a reliable method for studying fractal behavior, here robust detrended fluctuation analysis (r-DFAn), has provided an improved understanding of the factors that influence the fluctuation structure hydrological time series. Repeating this exercise using different hydrological models and for different sites, however, would help to support these results.

In addition, the issue of parameter interaction during calibration/optimization may be inferred from this study. Where certain combinations of parameters change may yield significant change to the fractal behavior of groundwater level. In particular, the change that the recharge parameters and the aquifer parameters had on the local fractal behavior of groundwater level where the former cause affects at smaller time scales whereas the latter caused affects at larger time scales.

ACKNOWLEDGMENTS

Mr James Sorensen and Dr John P Bloomfield publish with the permission of the Executive Director of the British Geological Survey (NERC).

We extend our gratitude to Ms Katie Muchan from the Centre for Ecology and Hydrology, Wallingford, United Kingdom, for making available for this work the meteorological data monitored at the Wallingford site.

DATA AVAILABILITY

The meteorological data can be requested from UK Centre for Ecology and Hydrology (UKCEH) from the following link: https://www.ceh.ac.uk/our-science/projects/wallingford-met-site and the river stage and groundwater level data, which are managed by the British

Geological Survey (BGS), can be downloaded from 10.5285/637eeed6-7175-4346-9321-0c14332456c6 (Sorensen, 2022)

REFERENCES

1. Allen, R. G., Pereira, L. S., Raes, D. & Smith, M. (1998) *Crop evapotranspiration: Guidlines for computing crop water requirements - FAO Irrigation and Drainage paper 56.* http://www.fao.org/docrep/x0490e/x0490e00.htm#Contents [Accessed August 2014].

2. Condon, L. & Maxwell, R. (2014) Groundwater-fed irrigation impacts spatially distributed temporal scaling behavior of the natural system: a spatio-temporal framework for understanding water management impacts. *Environmental Research Letters.* 9 (3), 034009.

3. Custódio, A. L., Madeira, J. F. A., Vaz, A. I. F. & Vicente, L. N. (2011) Direct multisearch for multiobjective optimization. *SIAM Journal on Optimization.* 21 1109-1140. https://www.mat.uc.pt/~lnv/papers/dms.pdf.

4. Duffy, C. J. & Gelhar, L. W. (1985) A Frequency Domain Approach to Water Quality Modeling in Groundwater: Theory. *Water Resources Research.* 21 (8), 1175-1184.

5. Duffy, C. & Gelhar, L. (1986) A Frequency Domain Analysis of Groundwater Quality Fluctuations: Interpretation of Field Data. *Water Resources Research.* 22 (7), 1115-1128.

6. Gelhar, L. W. (1974) Stochastic analysis of phreatic aquifers. *Water Resources Research.* 10 (3), 539-545. 10.1029/WR010i003p00539.

7. Habib, A. (2020) Exploring the physical interpretation of long-term memory in hydrology. *Stochastic Environmental Research and Risk Assessment.* 1-9. 10.1007/s00477-020-01883-0.

8. Habib, A., Sorensen, J. P. R., Bloomfield, J. P., Muchan, K., Newell, A. J. & Butler, A. P. (2017) Temporal scaling phenomena in groundwater-floodplain systems using robust detrended fluctuation analysis. *Journal of Hydrology.* 549 715-730.

9. Habib, A., Butler, A. P., Bloomfield, J. P. & Sorensen, J. P. R. (2022) Fractal domain refinement of models simulating hydrological time series. *Hydrological Sciences Journal.* 67 (9), 1342-1355. 10.1080/02626667.2022.2084342.

10. Istanbulluoglu, E., Wang, T., Wright, O. M. & Lenters, J. D. (2012) Interpretation of hydrologic trends from a water balance perspective: The role of groundwater storage in the Budyko hypothesis. *Water Resources Research.* 48 (3), n/a.

11. Kantelhardt, J. W., Koscielny-Bunde, E., Rego, H., Havlin, S. & Bunde, A. (2001) Detecting long-range correlations with detrended fluctuation analysis. *Physica A.* 295 (3-4), 441-454.
12. Katul, G. G., Porporato, A., Daly, E., Oishi, A. C., Kim, H., Stoy, P. C., Juang, J. & Siqueira, M. B. (2007) On the spectrum of soil moisture from hourly to interannual scales. *Water Resources Research.* 43 (5), n/a.
13. Li, Z. & Zhang, Y. (2007) Quantifying fractal dynamics of groundwater systems with detrended fluctuation analysis. *Journal of Hydrology.* 336 (1), 139-146.
14. Liang, X., Zhang, Y. & Schilling, K. (2016) Effect of heterogeneity on spatiotemporal variations of groundwater level in a bounded unconfined aquifer. *Stochastic Environmental Research and Risk Assessment.* 30 (1), 1-8.
15. Liang, X. & Zhang, Y. (2013) Temporal and spatial variation and scaling of groundwater levels in a bounded unconfined aquifer. *Journal of Hydrology.* 479 139-145. 10.1016/j.jhydrol.2012.11.044.
16. Little, M. A. & Bloomfield, J. P. (2010) Robust evidence for random fractal scaling of groundwater levels in unconfined aquifers. *Journal of Hydrology.* 393 (3), 362-369.
17. Lo, M. & Famiglietti, J. S. (2010) Effect of water table dynamics on land surface hydrologic memory. *Journal of Geophysical Research: Atmospheres.* 115 (D22), D22118.
18. Mandelbrot, B. B. (1982) *The fractal geometry of nature. [Primo]* New York, W. H. Freeman and Company.
19. Mathias, S. A., Skaggs, T. H., Quinn, S. A., Egan, S. C., Finch, L. E. & Oldham, C. D. (2015) A soil moisture accounting procedure with a Richards' equation-based soil texture-dependent parameterization. *Water Resources Research.* 51 (1), 506-523.
20. Matsoukas, C., Islam, S. & Rodriguez-Iturbe, I. (2000) Detrended fluctuation analysis of rainfall and streamflow time series. *Journal of Geophysical Research: Atmospheres.* 105 (D23), 29165-29172.
21. Molnar, P. & Burlando, P. (2008) Variability in the scale properties of high- resolution precipitation data in the Alpine climate of Switzerland. *Water Resources Research.* 44 (10), .
22. National Research Council. (1991) *Opportunities in the Hydrologic Sciences.* Washington, DC, The National Academies Press.
23. Over, T. M. (1995) *Modelling space-time rainfall at the mesoscale using random cascades.* University of Colorado.

24. Over, T. M. & Gupta, V. K. (1994) Statistical Analysis of Mesoscale Rainfall: Dependence of a Random Cascade Generator on Large-Scale Forcing. *Journal of Applied Meteorology.* 33 (12), 1526-1542.
25. Paschalis, A., Molnar, P. & Burlando, P. (2012) Temporal dependence structure in weights in a multiplicative cascade model for precipitation. *Water Resources Research.* 48 (1), .
26. Peng, C. K., Buldyrev, S. V., Havlin, S., Simons, M., Stanley, H. E. & Goldberger, A. L. (1994) Mosaic organization of DNA nucleotides. *Physical Review.E, Statistical Physics, Plasmas, Fluids, and Related Interdisciplinary Topics.* 49 (2), 1685.
27. Rahman, M., Sulis, M. & Kollet, S. J. (2016) Evaluating the dual- boundary forcing concept in subsurface– land surface interactions of the hydrological cycle. *Hydrological Processes.* 30 (10), 1563-1573.
28. Russian, A., Dentz, M., Borgne, T., Carrera, J. & Jimenez-martinez, J. (2013) Temporal scaling of groundwater discharge in dual and multicontinuum catchment models. *Water Resources Research.* 49 (12), 8552-8564.
29. Sorensen, J. (2022) *High resolution river stage and groundwater level data from Wallingford, Oxfordshire, UK. NERC EDS National Geoscience Data Centre.* 10.5285/637eeed6-7175-4346-9321-0c14332456c6.
30. Thompson, S. E. & Katul, G. G. (2011) Multiple mechanisms generate Lorentzian and 1/f^α power spectra in daily stream-flow time series. *Advances in Water Resources.*
31. Van Genuchten, M. T. (1980) A closed-form equation for predicting the hydraulic conductivity of unsaturated soils. *Soil Scince Society of America Journal.* 44 (5), 893.
32. Williams, Z. C. & Pelletier, J. D. (2015) Self-affinity and surface-area-dependent fluctuations of lake-level time series. *Water Resources Research.* 51 (9), 7258-7269.
33. Yang, C., Zhang, Y. & Liang, X. (2017) Analysis of temporal variation and scaling of hydrological variables based on a numerical model of the Sagehen Creek watershed. *Stochastic Environmental Research and Risk Assessment.*
34. Yu, X., Ghasemizadeh, R., Padilla, I. Y., Kaeli, D. & Alshawabkeh, A. (2016) Patterns of temporal scaling of groundwater level fluctuation. *Journal of Hydrology.* 536 485-495.
35. Zhang, Y. & Li, Z. (2006) Effect of temporally correlated recharge on fluctuations of groundwater levels. *Water Resources Research.* 42 (10), n/a.
36. Zhang, Y. & Schilling, K. (2004) Temporal scaling of hydraulic head and river base flow and its implication for groundwater recharge. *Water Resources Research.* 40 (3), .

TABLES

Table 1: Summary of the data measured at the study site from January 2012 – January 2016

Datasets	**Measuring Station**	**Time Resolution (minutes)**
Meteorological Data		
Rainfall	Automatic weather station (AWS)	15
Dry bulb temperature		15
Wet bulb temperature		15
Net solar radiation		15
Wind speed		15
Hydrological Data		
Groundwater levels	WL84	1
River Stage	Thames stilling well	1

Table 2: Summary of parameters used in the sensitivity analysis of the fractal behavior

Parameter Symbol	**Parameter Description**	**The range used for sensitivity analysis**
Stochastic Rainfall Model		
β	Intermittency parameter	Changes to parameter such that the resulting rainfall series exhibit scaling between 0.6 and 1.05
Recharge Parameters (from the Soil Moisture Accounting Recharge Model)		
m	Empirical parameter from the Van Genuchten-Maulem Model	Between 25 and 175% (i.e. multiplied by values between 0.25 and 1.75)
η	Empirical parameter from the Van Genuchten-Maulem Model	Between 25 and 175%
Aquifer Physical Parameters (from the 1D Boussinesq Eq Groundwater Flow Model)		

K	Hydraulic conductivity	Between 50 and 500% (i.e. multiplied by values between 0.5 and 5)
S_y	Specific yield	Between 50 and 500%
Other Parameters		
No symbol used	River stage fractal behavior	Two series used: first is original river stage series, second is randomly shuffled version with white noise scaling
No symbol used	Distance from river	At 420m (actual distance of boreholes from river), 300m, 200m, 100m, 50m and 25m

FIGURES

Figure 1: A Google Earth image of the study site in Wallingford, United Kingdom, with the automatic weather station (AWS), the Thames stilling well and the groundwater boreholes (WL84 and 85) indicated © Google Earth 2022.

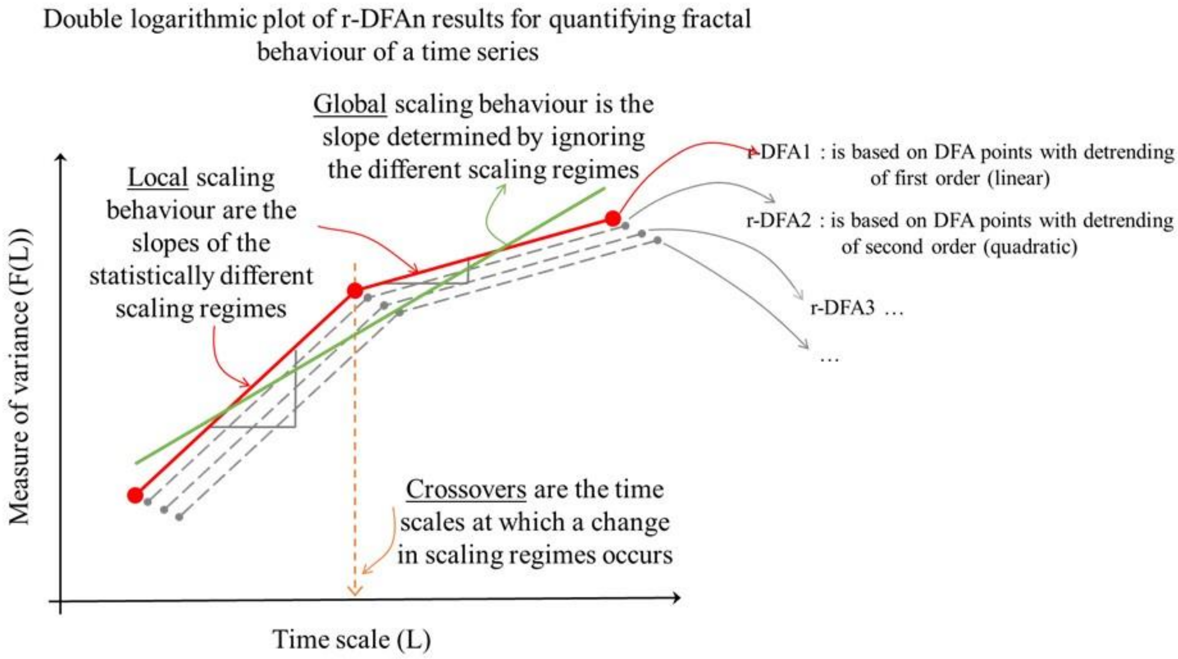

Figure 2. Explanation of the various components of fractal behavior that robust detrended fluctuation analysis (r-DFAn) quantifies.

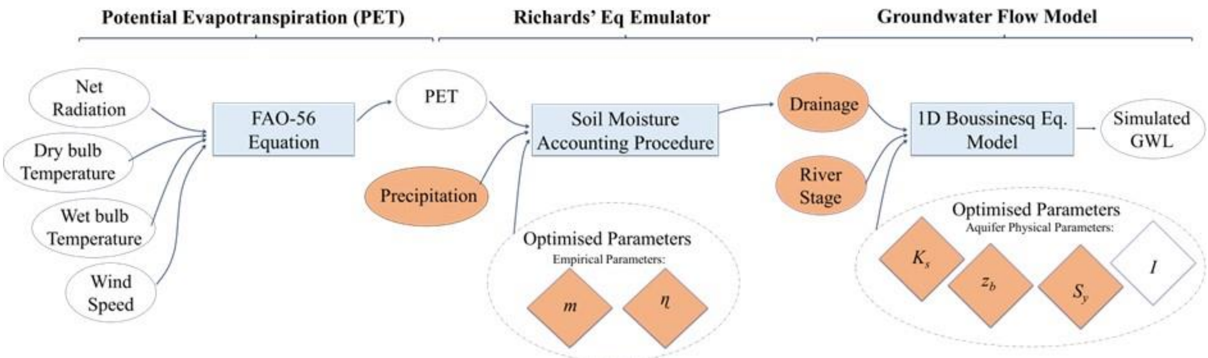

Figure 3. A schematic showing the input time series and sensitive parameters of the recharge-groundwater flow model. Ovals represent time series, diamond shapes represent sensitive parameters and rectangles represent an algorithm. Orange highlighted shapes are the parameters/time series that are involved in the sensitivity study of groundwater levels' fractal behavior. PET is potential evapotranspiration, m and η are empirical parameters from the recharge model (one value for summer and one for winter for each parameter), K_s is the hydraulic conductivity of the saturated zone, z_b is the elevation of the base of the aquifer from ordnance datum, S_y is the specific yield of the aquifer, and I is the constant inflow near the no-flow boundary.

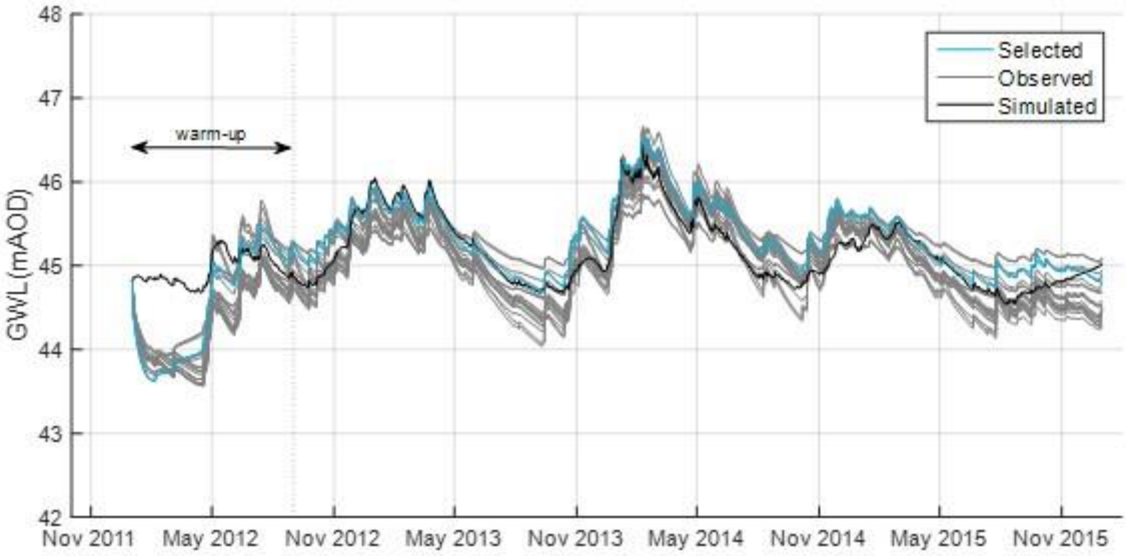

Figure 4. Simulated non-dominated groundwater levels (GWL) using the coupled recharge-groundwater flow model and observed GWL.

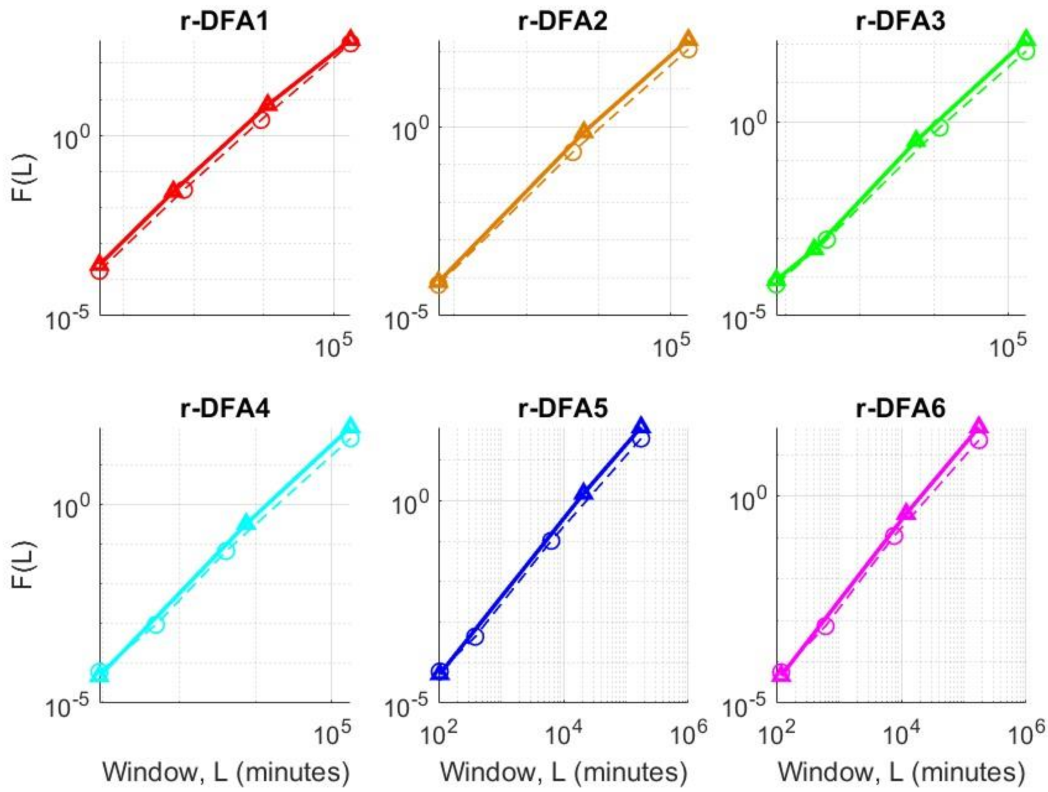

Figure 5. Fractal behavior of the selected groundwater levels simulation and how it compares to the fractal behavior of observed groundwater levels. The dashed lines are observed fractal behavior and the solid lines are the simulated fractal behavior.

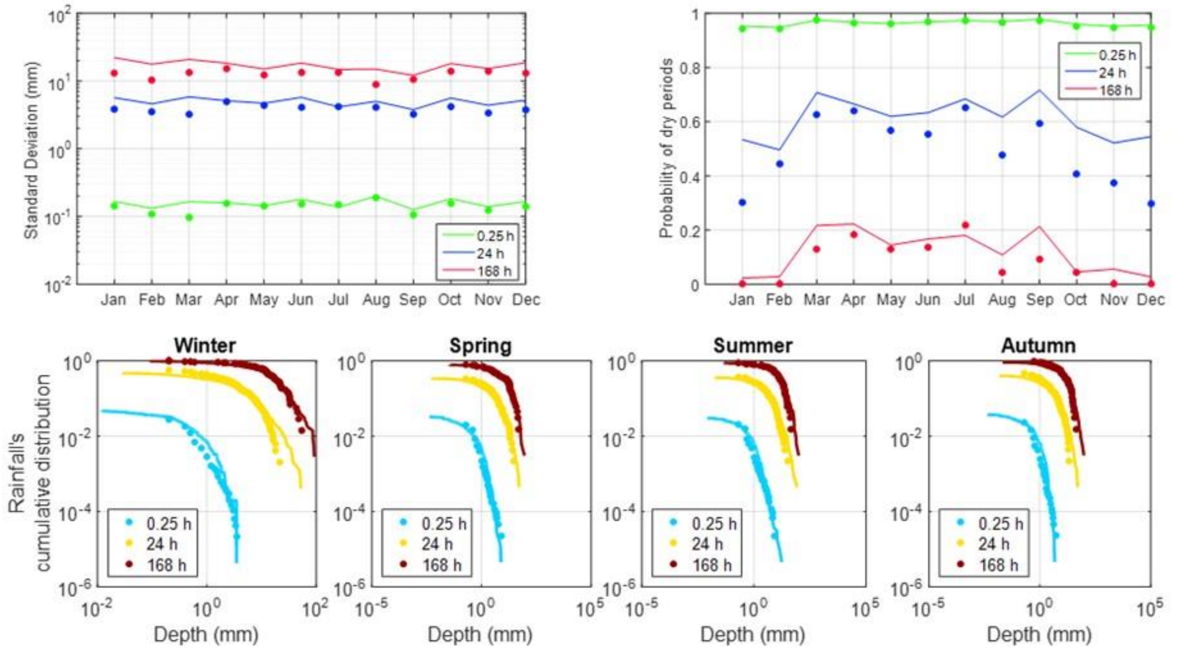

Figure 6. Top left: comparison between the standard deviations of each month of observed data (dots) and simulated rainfall (lines). Top right: comparison between the probability of dry periods of each month of observed data (dots) and simulated rainfall (lines). Bottom: comparison between empirically fitted cumulative distributions of observed data (dots) and simulated rainfall (lines) for each season. Three scales are selected for the model's performance assessment: 15 minutes, 1 day and 1 week

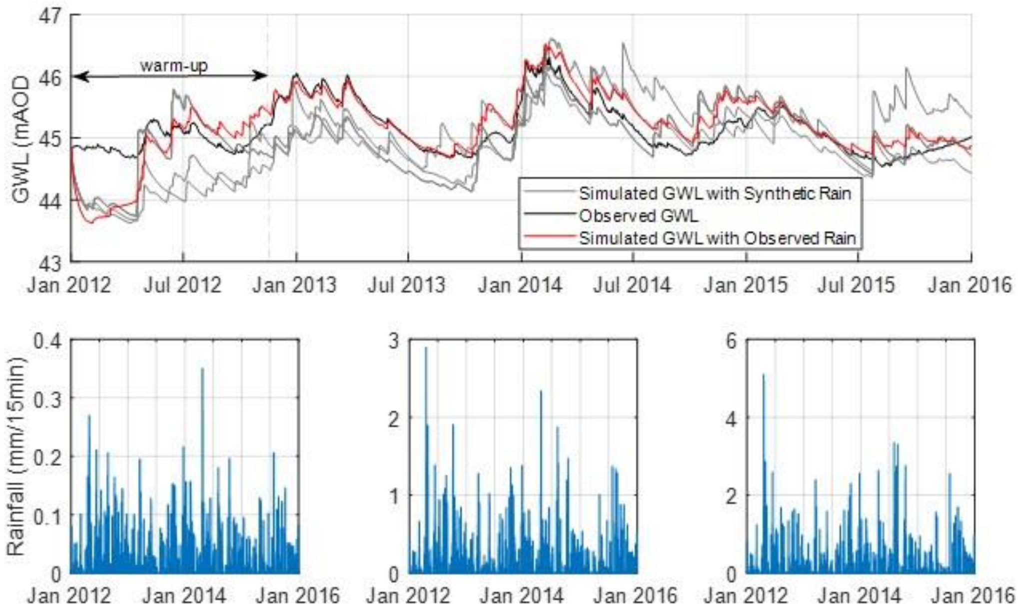

Figure 7. Top panel: groundwater levels simulated using observed rainfall and selected rainfall realisations. Bottom panels: selected rainfall realisations.

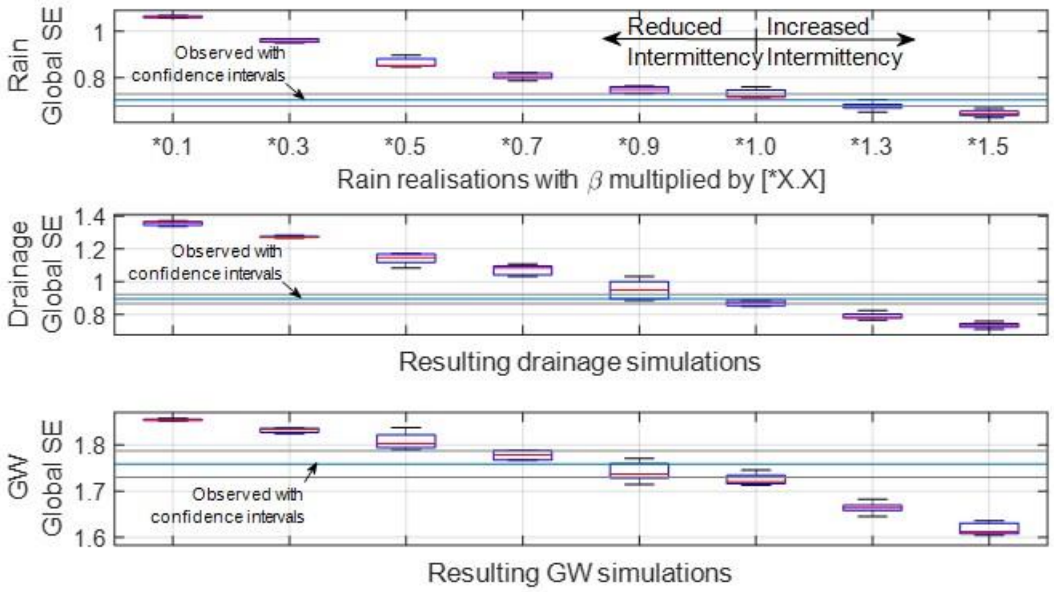

Figure 8. Box plots summarising the global scaling exponents of the 40 simulated rainfall realisations (top panel) and corresponding drainage (middle panel) and groundwater levels (bottom panel). The red line represents the median, box edges represent the 25th and 75th percentiles, whiskers represent the maximum range.

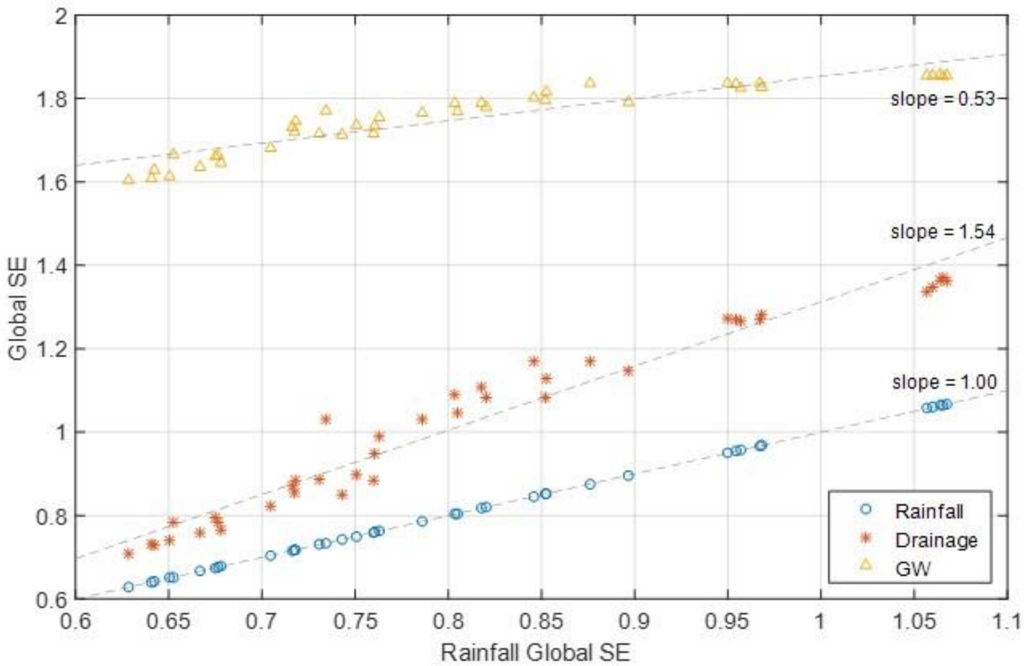

Figure 9. Scatter plot of simulated rainfall, drainage and groundwater levels' global fractal behavior vs. simulated rainfall's global fractal behavior

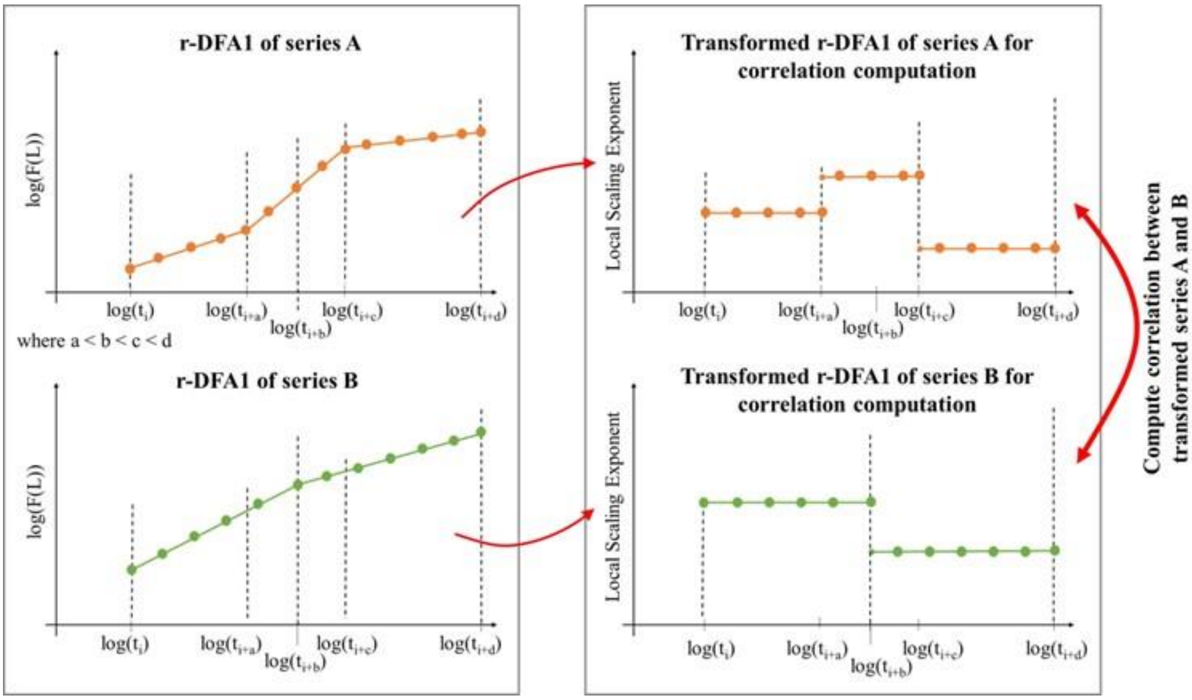

Figure 10. Illustration that explains how the r-DFA1 plots are transformed in order to be able to compute a correlation coefficient between pairs of r-DFA1 plots.

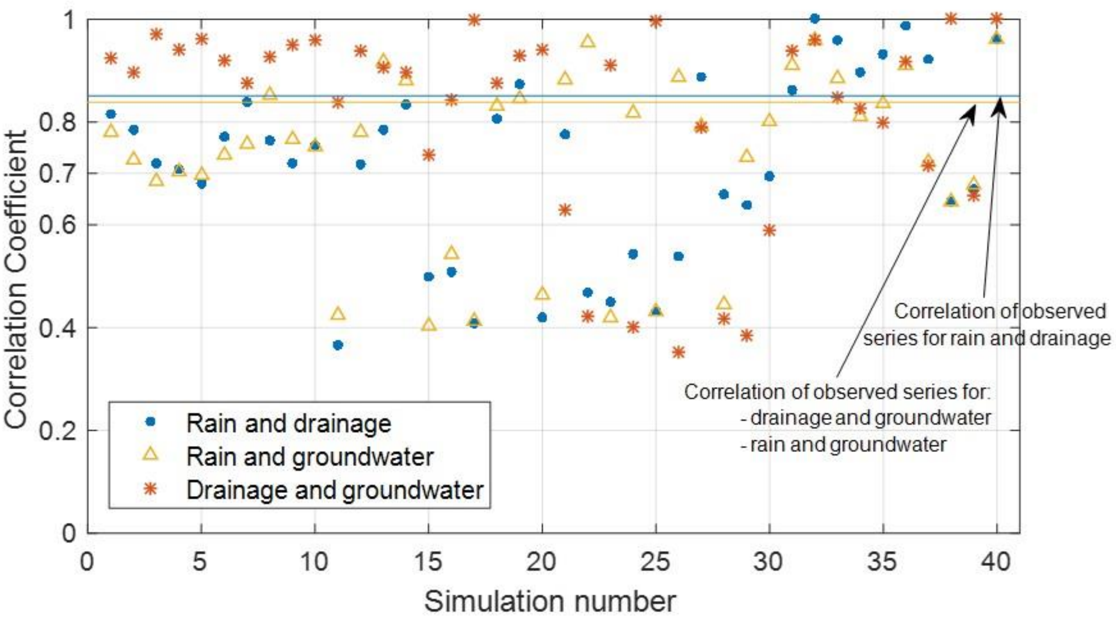

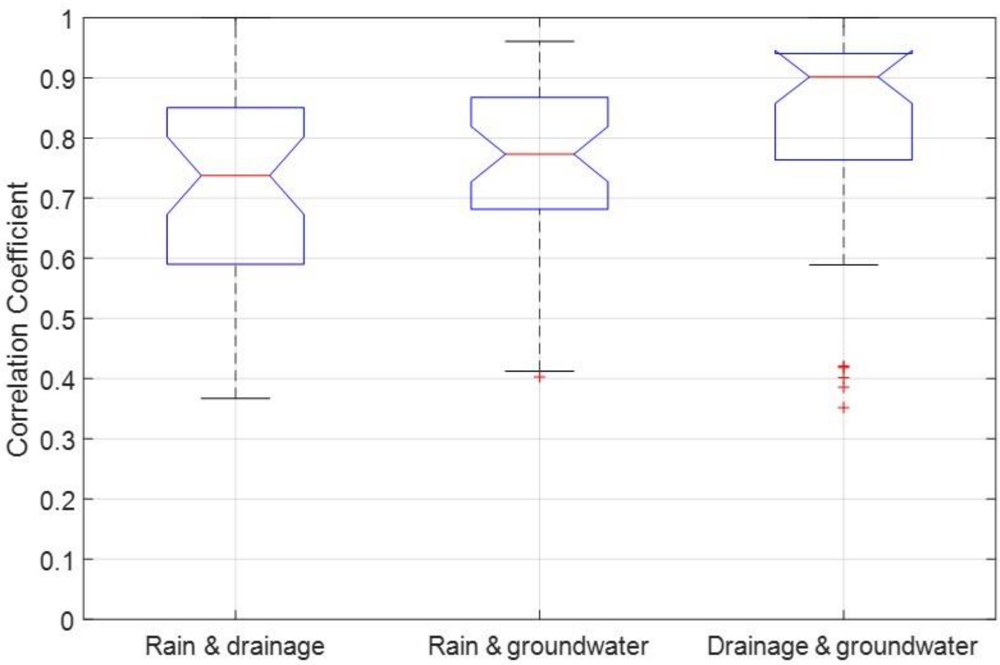

Figure 11. Top panel: correlations between the 40 realisations of rainfall, drainage and groundwater levels' local scaling exponents (r-DFA1). Bottom panel: Boxplots summarising the results presented in the top panel. The red line represents the median, notches represent the confidence intervals of the median with 95% significance level, box edges represent the 25th and 75th percentiles, red crosses represent outliers, and, whiskers represent the maximum range excluding the outliers.

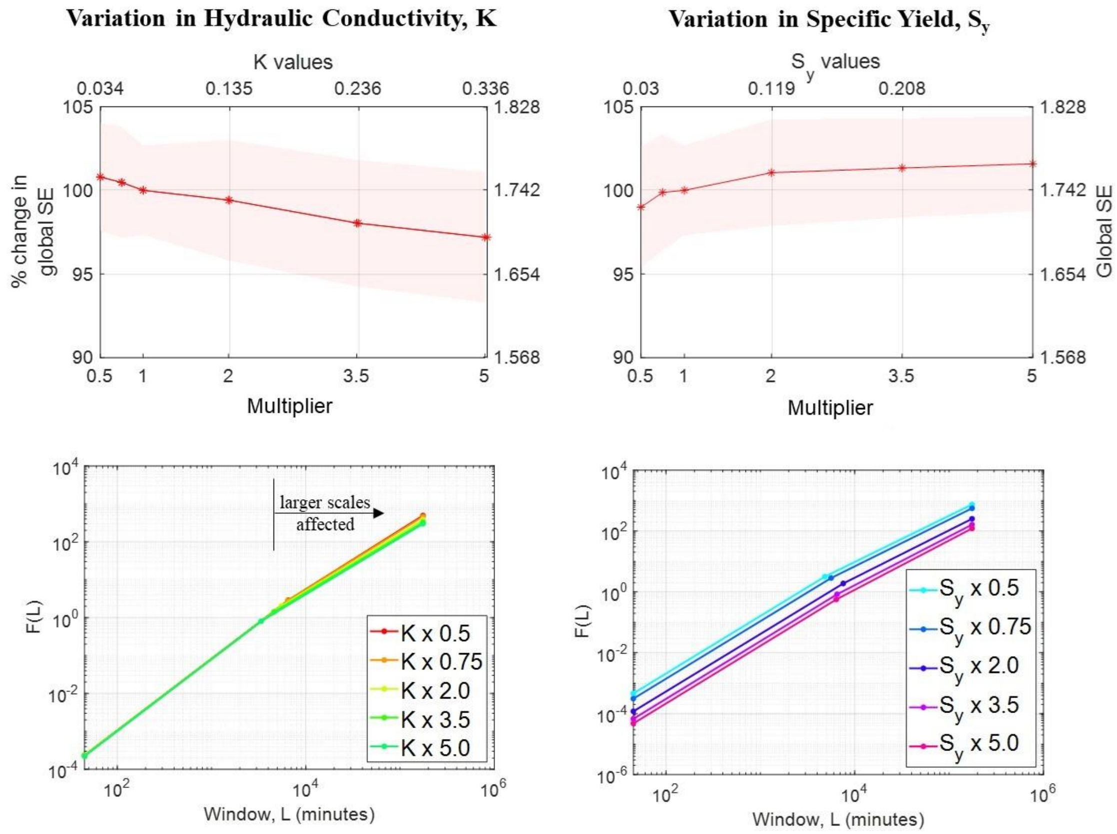

Figure 12. Top panels: Effect of change of hydraulic conductivity (left) and specific yield (right) on the global scaling exponent of simulated groundwater level with 95% confidence intervals. Bottom panels: r-DFA1 results of groundwater levels simulated with varying hydraulic conductivities and specific yield.

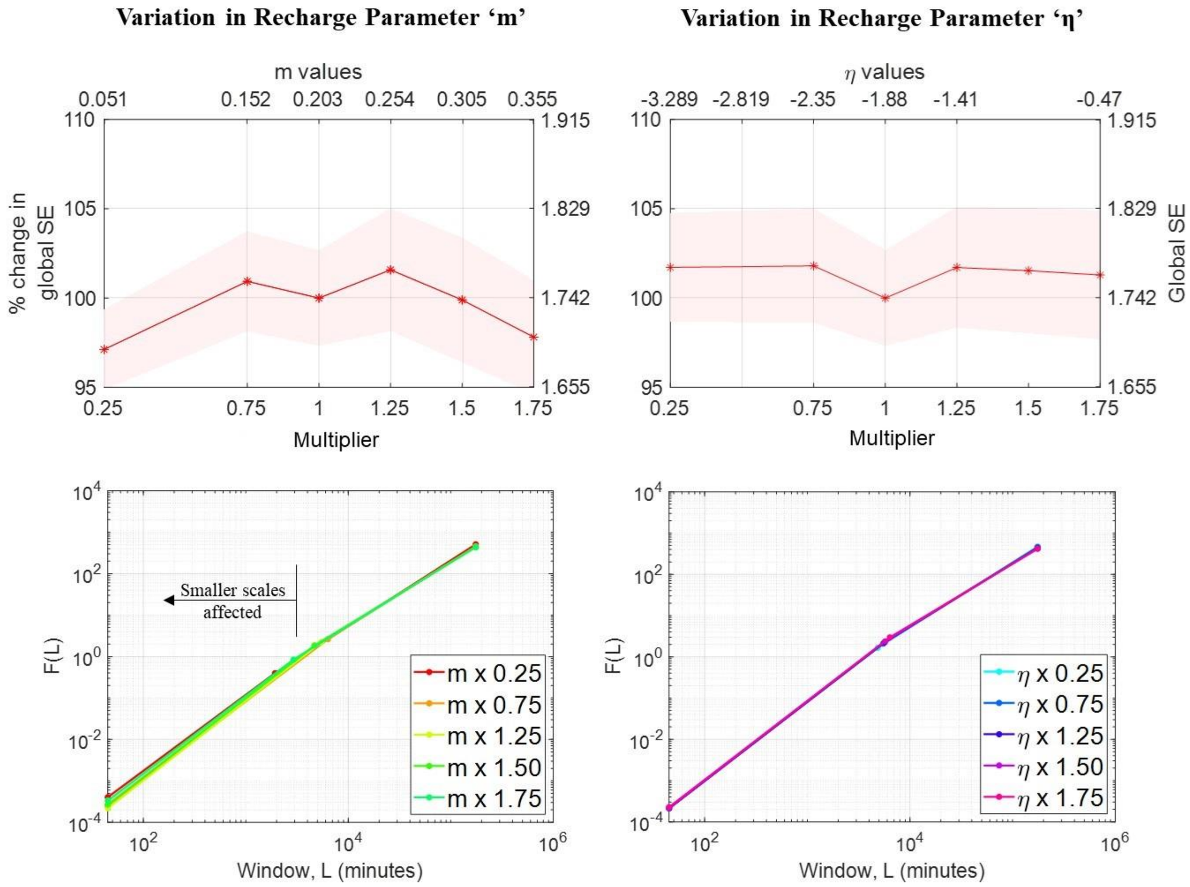

Figure 13. Top panel: Effect of change of different recharge parameter values on the global scaling exponent of simulated groundwater level with 95% confidence intervals. Bottom: r-DFA1 results of groundwater levels simulated with varying recharge parameter values.

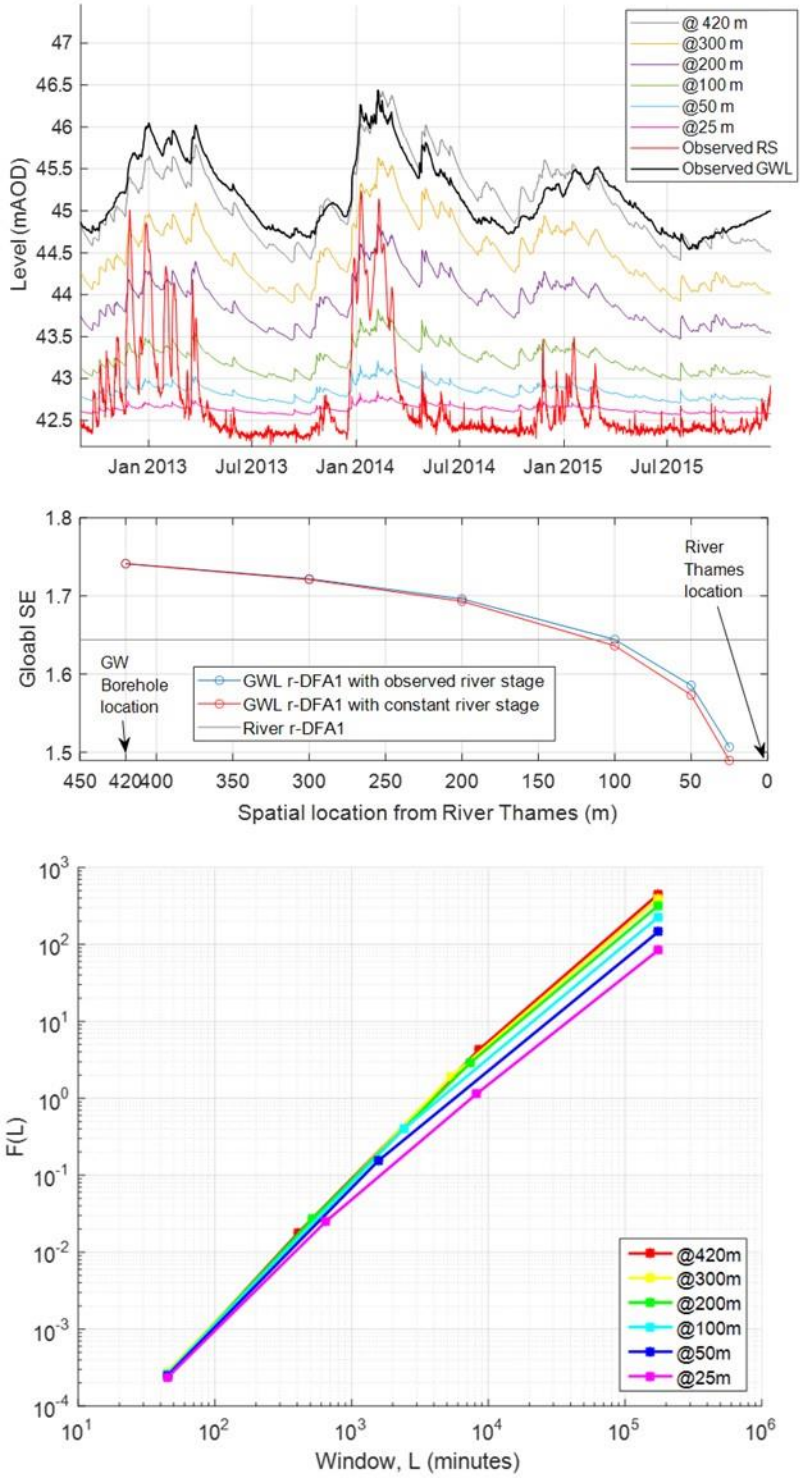

Figure 14. Top panel: Simulated groundwater time series at different locations. Middle Panel: Global fractal behavior of simulated groundwater levels at different locations with, first, observed river stage as boundary condition and then a constant (mean value) river stage as boundary condition. Bottom panel: Local scaling behavior of first order (i.e., r-DFA1) at different locations.